Electronic Supplementary Material

Preparation of MIL-68@Fe_3O_4@PVDF Composites via Spray Phase Inversion Method and Their Magnetic Solid-Phase Extraction of Parabens and Bisphenol A

Xinwen Hu[1], Yong Zhang[1], Zhihao Chen, Mengqian Xiao, Litao Wang, Guihua Gao*

[a] *School of Pharmacy*, *Shandong University of Traditional Chinese Medicine*, *Jinan* 250355 *Shandong Province*, *P. R. China*

[b] *School of Pharmacy*, *Jining Medical University*, *Rizhao* 276826 *Shandong Province*, *P. R. China*

*Correspondence: School of Pharmacy, Jining Medical University, Rizhao, Shandong Province, 276826, P. R. China

E-mail address:guihua526@163.com

Fax: +86-633-2983690

[1] These authors contributed equally to this work.

Content List

1. Synthesis of MIL-68(Al)

MIL-68(Al) was prepared by the reported method with minor modifications.[1] The specific synthesis steps are as follows: $AlCl_3 \cdot 6H_2O$ (44 g, 0.29 mol) was dissolved into 210 mL of isopropanol in a 500 mL PTFE-lined stainless steel autoclave. H_2BDC (6 g, 0.037 mol) was then added to the mixture under stirring. The mixture was then heated at 140℃ for 5 h. After cooling down to room temperature, the solution was removed by centrifugation. The obtained powder of MIL-68(Al) was washed thrice with ultrapure water and then washed with DMF under refluxing at 150℃ for 8 h. The product was then drenched in ethanol solution for 1 h three times to remove residual DMF. Finally, the obtained white MIL-68(Al) powders were dried under vacuum.

2. Synthesis of Fe_3O_4

Fe_3O_4 was synthesized based on a previously reported procedure with minor modifications.[2] Briefly, $FeSO_4 \cdot 7H_2O$ (1.40 g) and $FeCl_3 \cdot 6H_2O$ (1.70 g) were first dissolved separately in an appropriate volume of ultrapure water, the two solutions were then transferred to a 250 mL three-necked flask, and the total volume of the mixture was adjusted to 150 mL with additional ultrapure water. The mixture was magnetically stirred at 400 rpm and 40℃ for 30 min to ensure uniform mixing. Subsequently, ammonia water (1.91 mol/L) was added dropwise to the mixed solution until the pH reached 9, and the reaction was continued under the same stirring and temperature conditions for 1 h to complete the reaction. After that, the synthesized Fe_3O_4 particles were collected via magnetic separation, washed twice with ultrapure water followed by anhydrous ethanol to remove unreacted precursors and impurities, and finally vacuum-dried at 60℃ for 8 h to obtain black Fe_3O_4 powder. The powder was sieved through a 200-mesh sieve to ensure uniform particle size and stored in a desiccator for subsequent composite preparation.

3. Optimization of Preparation Conditions and Batch-to-Batch Reproducibility

3.1 Design of MIL-68@Fe_3O_4@PVDF

To develop a MSPE-suitable magnetic adsorbent, MIL-68@Fe_3O_4@PVDF was designed with three functional components: MIL-68(Al) (adsorption phase, for targets capture), Fe_3O_4 (magnetic phase, for rapid separation), and PVDF (binder, for structural stability). The composite was fabricated via spray phase inversion—an approach enabling one-step PVDF solidification and synchronous MIL-68(Al) loading, which simplifies synthesis compared to traditional multi-step methods. The MIL-68(Al):Fe_3O_4:PVDF mass ratio is critical for balancing the composite's MSPE-related performance. Sufficient Fe_3O_4 ensures fast magnetic separation, but excess Fe_3O_4 reduces MIL-68(Al) loading; optimized PVDF forms intact microspheres, while insufficient/overabundant PVDF causes brittleness or pore blockage; and adequate MIL-68(Al) guarantees adsorption capacity, though overloading leads to agglomeration. To screen this ratio, methylene blue (MB) was used as a model pollutant. The MB adsorption rate (AR, %) served as the key metric to guide subsequent experiments on each component's content.

To investigate the influence of MIL-68(Al) content on the adsorption performance of MIL-68@Fe_3O_4@PVDF, experiments were conducted with fixed masses of Fe_3O_4 (0.1 g) and PVDF (0.175 g), while varying the mass of MIL-68(Al). As shown in Fig. S1a, AR of MB exhibited a trend of first increasing and then decreasing with increasing MIL-68(Al) mass, reaching a maximum when the MIL-68(Al) mass was 0.15 g. This trend can be attributed to the dual role of MIL-68(Al) as the primary adsorption component. With increasing MIL-68(Al) content (0.05–0.15 g), more active sites become available for MB adsorption, directly enhancing the composite's adsorption capacity. However, when the MIL-68(Al) mass exceeded 0.15 g, the PVDF matrix—acting as the structural support—reached its maximum loading capacity. Excess MIL-68(Al) could not be effectively immobilized on the PVDF surface, leading to two adverse effects: unloaded MIL-68(Al) particles aggregated in the coagulation bath (reducing their utilization efficiency), and the overcrowded surface layer disrupted the spherical structure of PVDF microspheres, which in turn hindered mass transfer of MB to the adsorption sites. Given that the highest AR was achieved at 0.15 g MIL-68(Al), this mass was selected as optimal for subsequent composite preparation.

Fe_3O_4 is critical for endowing MIL-68@Fe_3O_4@PVDF with magnetic responsiveness—a core requirement for MSPE, as it directly dictates the efficiency of post-adsorption magnetic separation.

However, excessive Fe_3O_4 can exceed the PVDF matrix's effective doping capacity, disrupting the integrity of composite microspheres and undermining both the synthesis process and long-term performance stability. To optimize Fe_3O_4 content, experiments were conducted with fixed masses of MIL-68(Al) (0.15 g) and PVDF (0.175 g), while varying the mass of Fe_3O_4. As shown in Fig. S1b, the AR first increased and then decreased with increasing Fe_3O_4 mass, peaking when Fe_3O_4 reached 0.1 g. This trend can be attributed to the fact that an appropriate amount of Fe_3O_4 doped in PVDF may promote the formation of larger microspheres during phase inversion, thereby enhancing the loading capacity for MIL-68(Al). In contrast, when Fe_3O_4 exceeded 0.1 g, two issues emerged: the excess nanoparticles caused microsphere fragmentation and occupied binding sites on the PVDF surface that would otherwise anchor MIL-68(Al). This reduced the actual loading of MIL-68(Al)—the primary adsorption component—leading to a noticeable decline in AR. So 0.1 g of Fe_3O_4 was selected as optimal for composite preparation.

To optimize the PVDF dosage—critical for forming stable composite microspheres—the effect of PVDF content on adsorption performance was investigated with fixed masses of MIL-68(Al) (0.15 g) and Fe_3O_4 (0.1 g). As shown in Fig. S1c, the AR of MB first increased with increasing PVDF mass, reaching a maximum at 0.25 g, after which a gradual decline was observed. This trend stems from PVDF's role as a polymeric matrix: at lower PVDF contents, the matrix is insufficient to form a continuous, robust microsphere skeleton, leading to partial detachment of MIL-68(Al) and Fe_3O_4 during preparation. This reduces the number of exposed adsorption sites and lowers AR. When PVDF reaches 0.25 g, it provides optimal structural support—effectively immobilizing both MIL-68(Al) and Fe_3O_4, thus maximizing AR. However, excess PVDF (>0.25 g) coats the surface of MIL-68(Al), physically blocking the interaction between MB molecules and adsorption sites, which in turn decreases AR. So 0.25 g of PVDF was selected as optimal for composite preparation.

By integrating the optimization results of the three components, the optimal masses for composite preparation were determined as follows: MIL-68(Al) = 0.15 g, Fe_3O_4 = 0.10 g, and PVDF = 0.25 g, corresponding to a mass ratio of 3:2:5. This ratio balances magnetic responsiveness, structural stability, and adsorption capacity—meeting the core requirements of an efficient MSPE adsorbent.

To explore how the distribution of MIL-68(Al) in the composite affects adsorption performance, a co-doping method was additionally used to prepare MIL-68@Fe_3O_4@PVDF, alongside the surface-loading approach. For the co-doping method, equal masses of MIL-68(Al) (0.1 g) and Fe_3O_4 (0.1 g)

were uniformly dispersed in a PVDF/DMF solution (0.25 g PVDF dissolved in 15 mL DMF). This mixture was atomized and sprayed into a 50% ethanol coagulation bath, resulting in a composite where MIL-68(Al) and Fe_3O_4 were embedded within the PVDF matrix. To distinguish it from the surface-loaded composite (prepared via the spray phase inversion method described in Section 2.3), this co-doped material is denoted as MIL-68@Fe_3O_4@PVDF (Internal), while the surface-loaded counterpart—where MIL-68(Al) is primarily immobilized on the PVDF microsphere surface—is referred to as MIL-68@Fe_3O_4@PVDF (External).

The MB adsorption performance of pure MIL-68(Al), MIL-68@Fe_3O_4@PVDF (Internal), and MIL-68@Fe_3O_4@PVDF (External) was compared, with results shown in Fig. S1d. The AR followed the order: pure MIL-68(Al) > MIL-68@Fe_3O_4@PVDF (External) > MIL-68@Fe_3O_4@PVDF (Internal). This trend reveals two key insights: first, MIL-68@Fe_3O_4@PVDF (External) maintains adsorption performance comparable to pure MIL-68(Al) while gaining the critical advantage of magnetic responsiveness. Second, the lower AR of the (Internal) composite arises from its structural design—MIL-68(Al) embedded in the PVDF matrix is partially encapsulated by the polymer, which blocks access to active sites for MB molecules. In contrast, the (External) composite exposes MIL-68(Al) on the PVDF surface, preserving high accessibility of active sites.

Given its balanced adsorption performance and magnetic separability, MIL-68@Fe_3O_4@PVDF (External) was selected for all subsequent experiments. For brevity, it is referred to simply as "MIL-68@Fe_3O_4@PVDF" in the following sections.

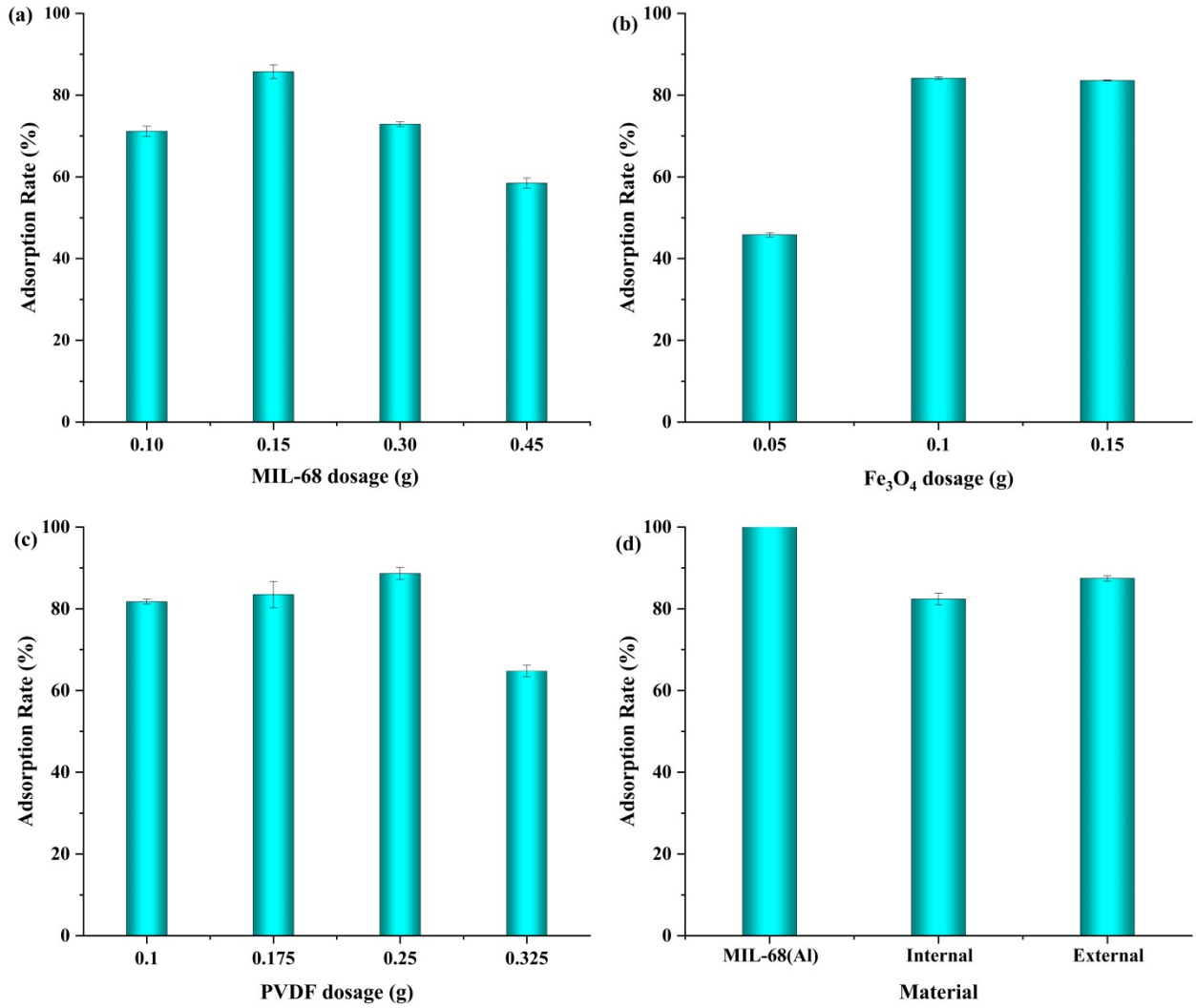

Fig. S1 Effect of MIL-68(Al) dosage (a), Fe_3O_4 dosage (b), PVDF dosage (c), and material (d) on the adsorption of MB by MIL-68@Fe_3O_4@PVDF

3.2 Batch-to-batch reproducibility

To evaluate the stability and reliability of the synthetic method, the batch-to-batch reproducibility of the composite was investigated using three independently prepared batches. All samples were sieved through a 200-mesh sieve to ensure particle size consistency. Using MB as the target analyte, the adsorption efficiency of each batch was determined. The adsorption efficiencies of the three batches were 88.94%, 88.87%, and 90.13%, respectively, with RSD of 0.71%, suggesting good batch-to-batch reproducibility. These results demonstrated that the developed synthetic route was reproducible and feasible, which is favorable for its further application.

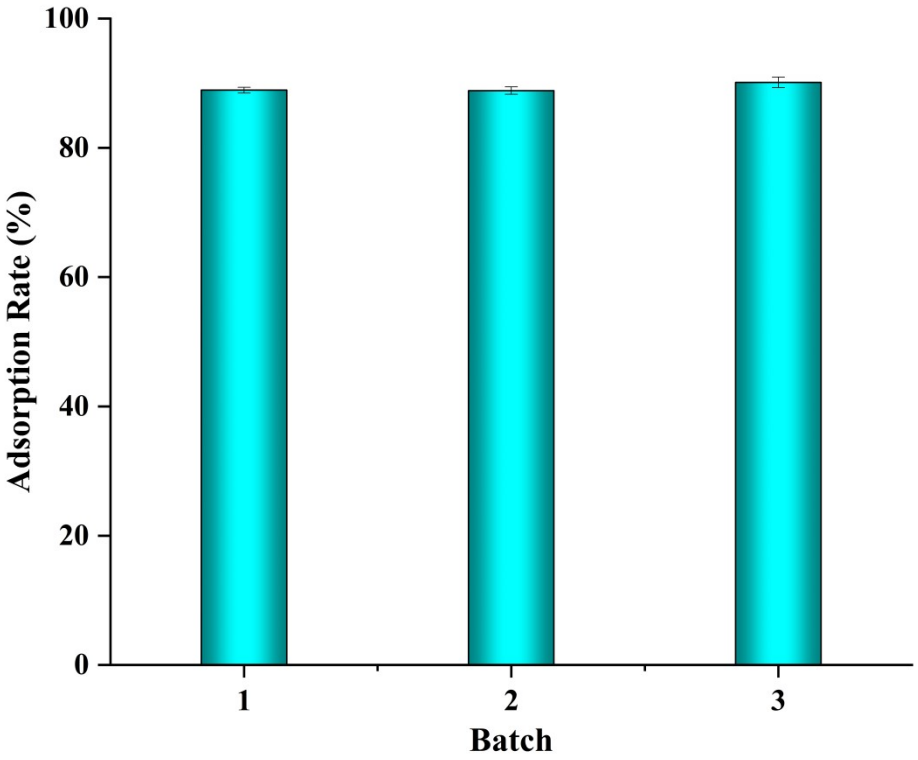

Fig. S2 Batch-to-batch repeatability of MIL-68@Fe_3O_4@PVDF.

4. Characterization of MIL-68@Fe_3O_4@PVDF

4.1 Fourier transforms infrared (FT-IR) spectroscopy

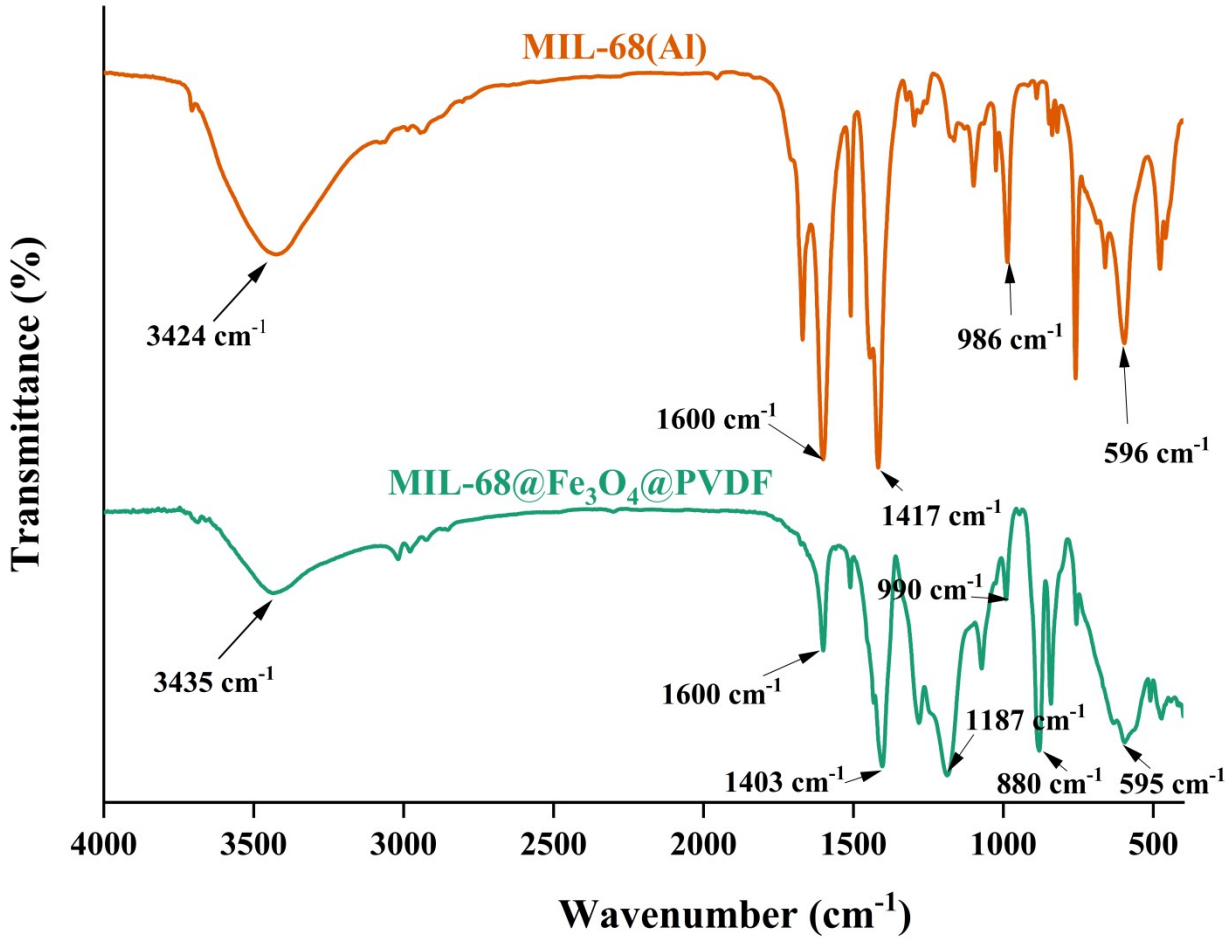

Fig. S3 FT-IR spectra of MIL-68(Al), and MIL-68@Fe_3O_4@PVDF.

4.2 N_2 Adsorption-Desorption Isotherms and Pore Structure Characterization

The specific surface area and pore structure characteristics of MIL-68(Al) and the MIL-68@Fe_3O_4@PVDF magnetic composite were systematically investigated via N_2 adsorption-desorption isotherms and Barrett-Joyner-Halenda (BJH) pore size distribution analysis (Fig. S4a–b). MIL-68(Al) exhibits a typical type I isotherm, characterized by a sharp adsorption uptake at low relative pressure ($P/P_0 < 0.1$), followed by a broad adsorption plateau at higher relative pressures, indicating a predominantly microporous structure. Correspondingly, the BJH pore size distribution curve shows a sharp characteristic peak at approximately 3–5 nm, further confirming the presence of uniform micropores, which is in good agreement with the typical structural features of MIL-68 series materials.[3] In contrast, the MIL-68@Fe_3O_4@PVDF magnetic composite exhibits a significantly reduced N_2 adsorption capacity over the entire pressure range. Its isotherm shows a gentle upward trend at higher relative pressures, and the pore size distribution undergoes pronounced changes: the intensity of the micropore peak is substantially suppressed, accompanied by the emergence of a broad and weak mesopore feature centered in the range of 10–20 nm.

The marked decrease in the Brunauer-Emmett-Teller (BET) specific surface area of the composite is primarily attributed to two factors: the dilution effect of the non-porous Fe_3O_4 nanoparticles, and the partial blockage of the intrinsic micropores of MIL-68(Al) by the polyvinylidene fluoride (PVDF) binder. Despite the reduced specific surface area, the material retains a hierarchical pore structure consisting of residual micropores, interparticle mesopores, and macropores within the PVDF matrix, which provides a structural basis for maintaining satisfactory adsorption performance. Meanwhile, Fe_3O_4 endows the composite with excellent magnetic responsiveness (facilitating rapid magnetic separation), while PVDF enhances its mechanical stability and processability, making the composite a promising candidate for adsorption separation applications.

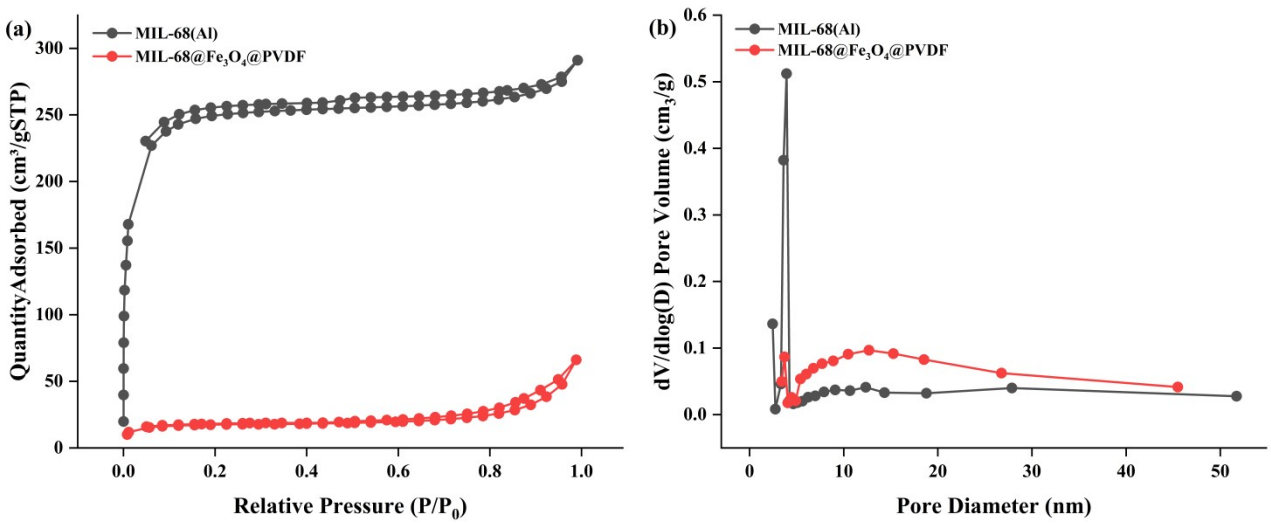

Fig. S4 (a) N_2 adsorption-desorption isotherms and (b) BJH desorption dV/dlog(D) pore size distribution curves of MIL-68(Al) and MIL-68@Fe_3O_4@PVDF.

5. Calibration curves of MB solution at different pH

A stock solution of methylene blue (MB) (1 mg/mL) was prepared and diluted with ultrapure water to obtain five standard solutions with concentrations of 0.001, 0.005, 0.010, 0.015, and 0.020 mg/mL. The pH of each MB solution was adjusted to values between 1 and 10 using 0.1 mol/L HCl or 0.1 mol/L NaOH. The absorbance of the MB solutions was measured at 663 nm using a microplate reader. Calibration curves were established by least squares linear regression of absorbance (y) against concentration (x).

Table S1 Calibration curves of MB solution at different pH

C (mg/mL)	pH	λ (nm)	calibration curve	*r*
0.001-0.020	1	663	y = 140.48x - 0.0455	0.9990
	2	663	y = 114.61x + 0.029	0.9996
	3	663	y = 117.1x + 0.0173	0.9995
	4	663	y = 117.75x + 0.0093	0.9999
	5	663	y = 121.57x + 0.0093	0.9995
	6	663	y = 112.83x - 0.0011	0.9998
	7	663	y = 112.02x - 0.0066	0.9999
	8	663	y = 116.85x - 0.03	0.9998
	9	663	y = 108.39x + 0.0054	0.9998
	10	663	y = 108.26x + 0.0114	0.9996

6. Adsorption optimization

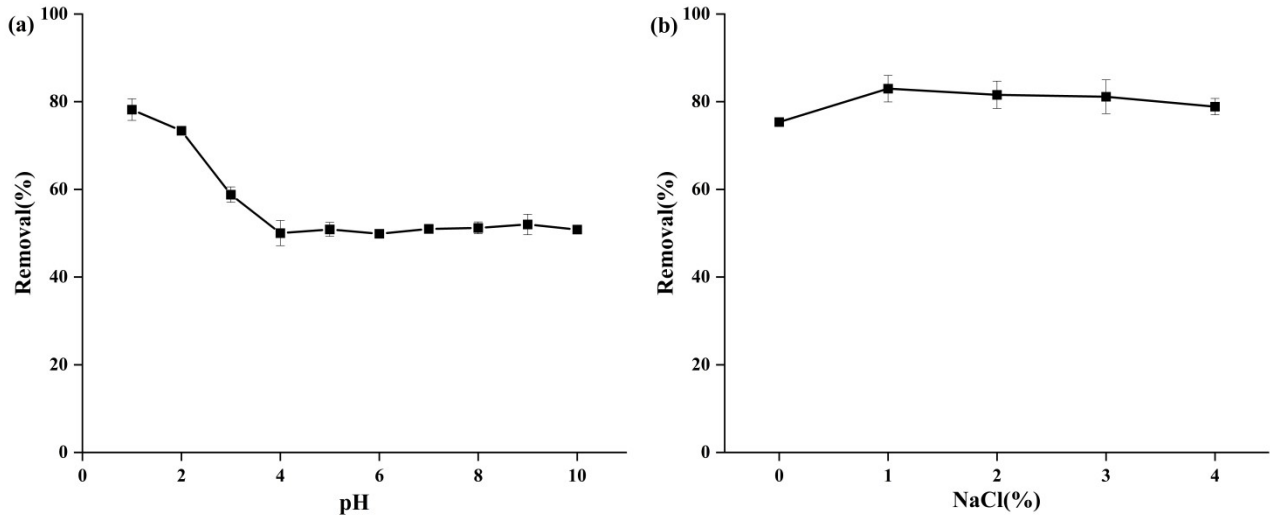

Fig. S5 Effects of pH and ionic strength on MB adsorption onto MIL-68@Fe_3O_4@PVDF: (a) pH; (b) ionic strength.

7. Adsorption kinetics

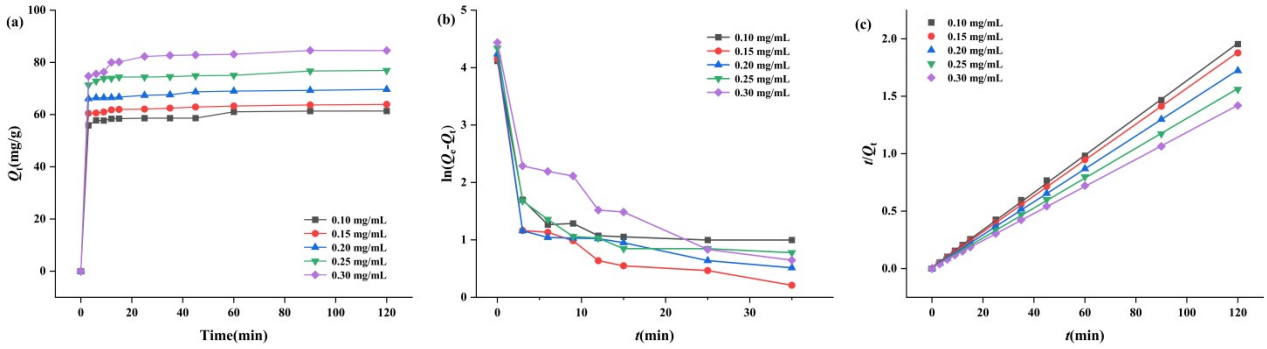

Fig. S6 Adsorption kinetics of MB on MIL-68@Fe_3O_4@PVDF: (a) Adsorption curve; (b) Pseudo-first-order kinetic plot; (c) Pseudo-second-order kinetic plot.

Table S2 Fitting parameters of adsorption kinetic models for the adsorption of MB onto MIL-68@Fe_3O_4@PVDF

Analyte	C_0(mg/mL)	$Q_{e,exp}$ (mg/g)	pseudo-first order model			pseudo-second order model		
			k_1 (min^{-1})	$Q_{e,cal}$ ($mg \cdot g^{-1}$)	r	k_2 （g/mg·min）	$Q_{e,cal}$ (mg/g)	r
MB	0.10	60.75	-0.0391	7.85	0.5731	0.0164	60.98	0.9999
	0.15	64.51	-0.0381	7.33	0.5450	0.0155	64.52	0.9998
	0.20	70.48	-0.0382	8.41	0.5552	0.0142	70.42	0.9998
	0.25	73.63	-0.0476	7.36	0.6053	0.0136	73.53	0.9999
	0.30	83.96	-0.0483	12.92	0.6644	0.0119	84.03	0.9998

8. Adsorption isotherms

Table S3 Fitting parameters of adsorption isotherm models for MB onto MIL-68@Fe_3O_4@PVDF

Analyte	Langmuir			Freundlich			Temkin		
	Q_m （mg/g）	K_L （L/mg）	r	K_F (mg/g(L/mg)$^{1/n}$)	n	r	A	B	r
MB	88.50	0.113	0.9840	41.15	7.41	0.8580	0.09874	9.49	0.8392

9. Analytical performance of the present method

Table S4 Analytical performance of the present method

Analyte	Spiked (ng/mL)	Intra-day precision (RSD, n=6)	Inter-day precision (RSD, n=6)	Repeatability (RSD, n=6)
MP	20	2.67	3.41	1.84
EP	10	3.04	2.51	2.13
PP	10	1.06	2.80	4.84
BPA	20	3.23	1.54	2.13
BP	20	2.49	2.16	2.05
BeP	50	2.94	1.50	0.98

10. HPLC-UVD chromatograms of standard solution, and water sample

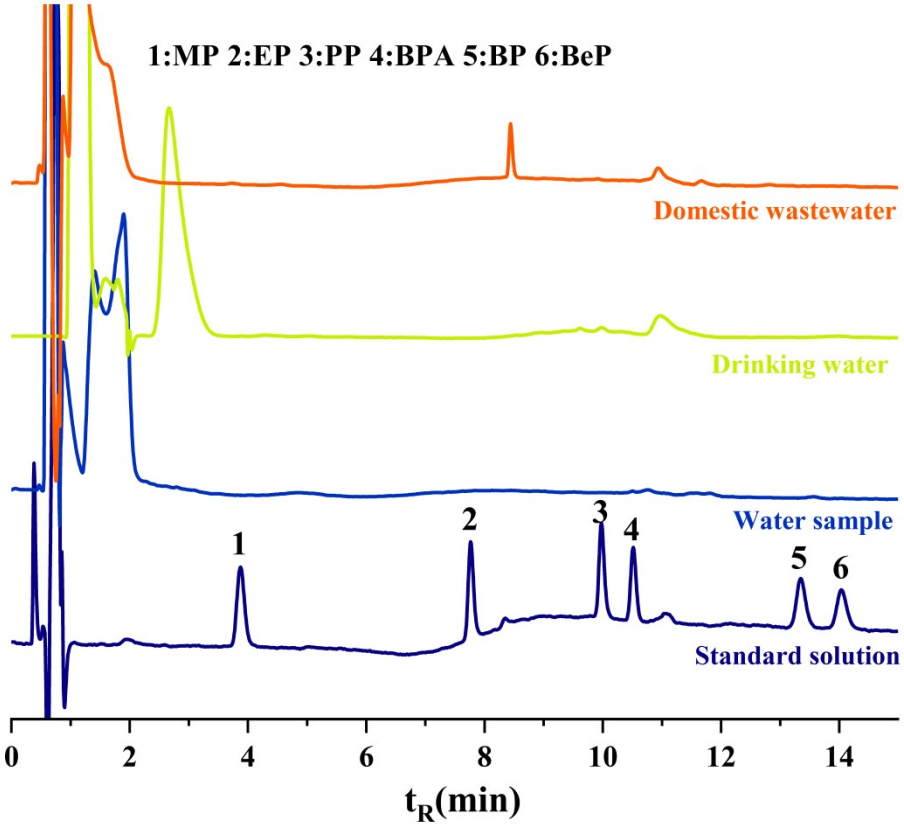

Fig. S7 Typical HPLC chromatograms of standard solution, drinking water, and domestic wastewater after MSPE.

11. Recyclability of MIL-68@Fe_3O_4@PVDF

The reusability and long-term stability of the as-prepared MIL-68@Fe_3O_4@PVDF composite were assessed by evaluating its extraction performance for six target analytes (MP, EP, PP, BPA, BP, and BeP) over repeated adsorption-desorption cycles under the optimal conditions (Fig. S8). The composite sustained high extraction efficiency across all cycles. After three consecutive cycles, a modest decline in recoveries occurred; nevertheless, the composite continued to exhibit satisfactory extraction performance for most of the target analytes. These observations indicate that the composite possesses both structural stability and good reusability, suggesting its applicability for the analysis of real water samples.

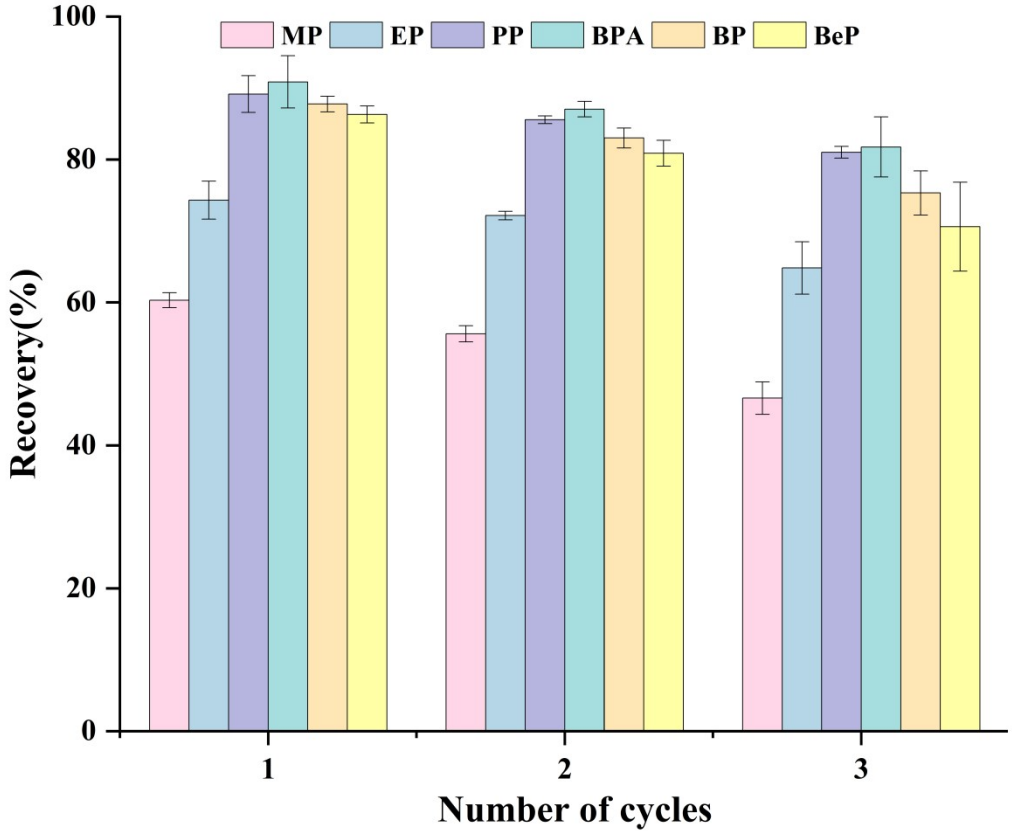

Fig. S8 Reusability study of the MIL-68@Fe_3O_4@PVDF.

12. Reference

[1]Q. Y. Yang, S. Vaesen, M. Vishnuvarthan, et al, Journal of Materials Chemistry, 2012, 22, 10210-10220.

[2]R. Massart, IEEE Transactions on Magnetics, 1981, 17, 1247-1248.

[3]M. S. Tehrani, R. Zare-Dorabei, Spectrochimica Acta Part A: Molecular and Biomolecular Spectroscopy, 2016, 160, 8-18.